Physics-Based Simulation of 1/*f* Noise in MOSFETs under Large-Signal Operation

Sung-Min Hong, Hong-Hyun Park, Chan Hyeong Park,* Myoung Jin Lee, Hong Shick Min and Young June Park
School of EECS and Nano-System Institute (NSI-NCRC), Seoul National University, Seoul 151-744, Korea
***Dept. of Electronics and Communications Eng., Kwangwoon University, Seoul 139-701, Korea**

Abstract

1/*f* noise in MOSFETs under large-signal excitation, which is important in CMOS analog and RF circuits, is modeled as a perturbation in the semiconductor equations employing both the oxide-trapping model and Hooge's model. The oxide-trapping model for a MOSFET in periodic large-signal operation shows that 1/*f* noise reduces more than conventional circuit simulation tools predict as the gate OFF voltage decreases further below the threshold voltage.

1. Introduction

Analysis of 1/*f* noise in MOSFETs has been typically carried out for MOSFETs in small-signal operation, where only DC biases are imposed on the device electrodes. Experimental results (for example [1]) for the drain noise current under the large signal operation show that the estimate using the small-signal noise model is much lower than the estimate using the small signal 1/*f* noise model. In this paper, we present a numerical framework, which is based on the CLESICO system [2], to model the 1/*f* noise under the large signal operation as well as the small operation regime.

2. Oxide-Trapping Model

Figure 1 shows the energy band diagram that illustrates considered carrier transition processes at the interface and in the oxide. The electron continuity equation, the interface trap continuity equation, and the oxide trap continuity equation can be written as follows:

$$\int_{\Omega_{\text{int}}} d\mathrm{a}\cdot \mathrm{J}_n = q\int_{A_{\text{int}}} da\left(\tfrac{\partial}{\partial t}n + r_{n,\text{int}} - g_{n,\text{int}}\right), \qquad (1)$$

$$0 = q\int_{A_{\text{int}}} da\left(\tfrac{\partial}{\partial t}n_{t,\text{int}} - r_{n,\text{int}} + g_{n,\text{int}} + r_{\text{int},ox} - g_{\text{int},ox}\right), \qquad (2)$$

$$0 = q\int_{\Omega_{ox}} dr\,\tfrac{\partial}{\partial t}n_{t,ox} + q\int_{A_{\text{int}}} da\left(-r_{\text{int},ox} + g_{\text{int},ox}\right), \qquad (3)$$

In the above equations, Ω_{int} is the control volume whose surface includes the interface, A_{int} is the interface, and Ω_{ox} is the control volume of an oxide node where oxide traps are located, as shown in Fig. 2.

Since the trap centers at the interface and in the oxide are distributed in both energy and space domains, a discretization in both variables is needed. We discretize a selected energy range in the oxide bandgap with small energy interval ΔE to account for the trap states which are related to 1/*f* noise, as shown in Fig. 3. Computationally expensive, this implementation gives accurate results. To alleviate the computational complexity, though, we employ the quasi-static approximation of the trapped electron density in the interface trap. Since we calculate the self-consistent solutions of Poisson's equation and the continuity equations, the Poisson effect of the trapped electron in the oxide trap is naturally included in our simulation.

Figure 4 shows a cross-sectional view of the MOSFET considered in this work. An 'oxide trap region' box in the figure indicates a region where the oxide trap levels are discretized. Parameters used in simulation are summarized in Tab. 1. Oxide trap density per unit energy is assumed to be uniform in both energy and space.

We first calculate the power spectral density of the drain noise current when the MOSFET is in the small-signal operation. Figure 5 shows the simulated power spectral density of the drain noise current at the gate voltage of 0.6 V as a function of frequency. The oxide-trapping noise with the uniform oxide trap density shows pure 1/*f* noise spectrum. Figure 6 shows the simulated power spectral density of the drain noise current at 10 Hz as a function of the gate bias voltage. Figure 7 shows the real part of the drain current Green's function for the oxide trap continuity equation in the oxide trap region. From the shape of the drain current Green's function, we can find that the oxide trap continuity equation can be approximated by an equation for a simple RC circuit, whose R value increases exponentially as the depth from the interface increases.

Now we calculate the power spectral density of the drain noise current when the MOSFET is in large-signal operation. We consider a periodically-switched MOSFET. Since our aim is to simulate the experimental set-up [1], the gate bias voltage is driven by a square-wave signal with 50 % duty cycle, as shown in Fig. 8. The harmonic balance simulation for the periodic steady-state is carried out including 12 harmonics plus DC, leading to 25 collocation points. In this case, the small-signal 1/*f* noise model predicts a noise power reduction by 6 dB.

Figure 9 shows the simulated power spectral densities of the drain 1/*f* noise current as a function of frequency for four OFF gate voltages of 0.5 V, 0.4 V, 0.3 V, and 0.1 V where the threshold voltage is 0.5 V. To further analyze the 1/*f* noise dependence on the OFF voltage levels, a noise reduction factor for different OFF voltages is plotted in Fig. 10. Additional noise reduction over 6 dB is observed for lower OFF voltages. The conversion Green's function [3] (from baseband to baseband) for the oxide trap continuity equation is shown for the OFF voltage of 0.1 V in Fig. 11. Figures 12 and 13 show the trap occupancies at 0.05 msec for the OFF voltages of 0.5 V and 0.1 V, respectively. From these figures, we notice that additional noise reduction over 6 dB comes from the reduction of the oxide trapping occupancy.

3. Hooge's Model

The same NMOSFET used in the oxide-trapping model, is simulated without the oxide traps. The noise reduction factor for different OFF voltages, which is calculated using Hooge's model [4], is plotted in Fig. 14. In this simulation, we employ a constant Hooge's parameter. Additional noise reduction over 6 dB is not observed for the lower OFF voltages.

The conversion Green's function (from baseband to baseband) for the electron continuity equation is shown for the OFF voltage of 0.1 V in Fig. 15. Since the conversion Green's function does not change for different OFF voltages, only the modulation of Hooge's noise sources plays an important role in Hooge's model for 1/*f* noise of MOSFETs in large-signal regime.

4. Conclusion

1/*f* noise in MOSFET in large-signal operation was modeled using both the oxide-trapping model and Hooge's model. In the oxide-trapping model, additional noise reduction over 6 dB was observed for the low OFF voltages. Additional noise reduction over 6 dB is due to the reduction of the oxide trapping occupancy. In Hooge's model, additional noise reduction over 6 dB was not observed for the low OFF voltages. Hooge's parameter for the MOSFET can not be an instantaneous function of the device operating point. It should contain the information about the periodic device operation. We expect that the approach described here can be applied to the physics-based phase noise simulation of oscillators, where $1/f$ noise source in MOSFETs is included [5].

References

[1] A. P. van der Wel, et al., IEEE EDL, vol. 21, pp. 43 - 46, 2000.
[2] S.-M. Hong, et al., SISPAD, pp. 119-122, 2005.
[3] F. Bonani, et al., IEEE TED, vol. 48, pp. 966-977, 2001.
[4] F. N. Hooge, IEEE TED, vol. 41, pp. 1926-1935, 1994.
[5] S.-M. Hong, et al., IEEE TED, vol. 53, pp. 2195-2201, 2006.

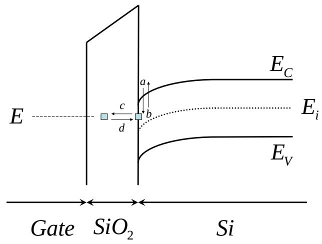

Fig. 1: Energy band diagram that illustrates considered carrier transition processes at the interface and in the oxide.

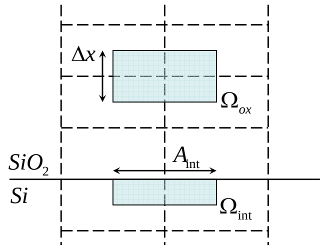

Fig. 2: Spatial discretization of the MOSFET.

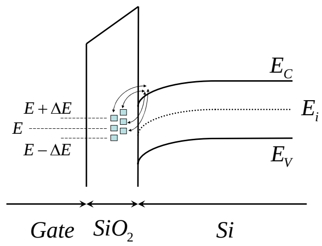

Fig. 3: Energy band diagram that illustrates the direct transition between the conduction band and the oxide traps under the quasi-static assumption of the trapped electron density in the interface trap.

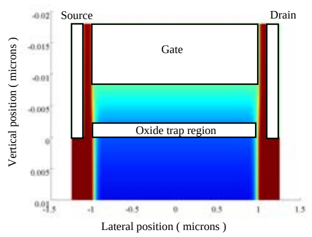

Fig. 4: Cross-sectional view of the MOSFET under simulation. The ‘oxide trap region’ box indicates the region where the oxide trap levels are discretized.

Oxide trap density	4×10^{17} cm^{-3} eV^{-1}
Interface trap density	10^{11} cm^{-2} eV^{-1}
Tunneling coefficient at interface	1.0 cm^{2} sec^{-1}
Tunneling attenuation coefficient	Trapezoidal barrier approximation

Tab. 1: Parameters used in simulation.

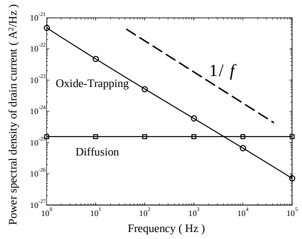

Fig. 5: Simulated power spectral density of the drain noise current at the gate voltage of 0.6 V as a function of frequency.

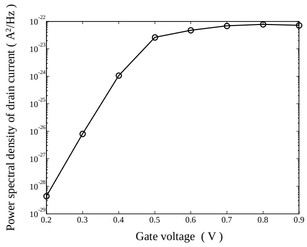

Fig. 6: Simulated power spectral density of the drain noise current at 10 Hz as a function of the gate bias voltage.

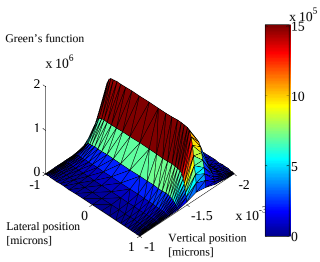

Fig. 7: Real part of the drain current Green’s function for the oxide trap continuity equation in the oxide trap region.

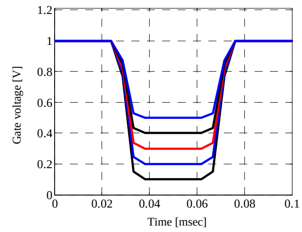

Fig. 8: The gate bias voltage is driven by a square-wave signal with 50 % duty cycle.

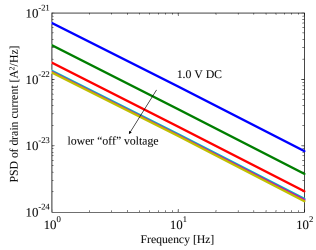

Fig. 9: Simulated power spectral density of the drain $1/f$ noise current as a function of frequency for four OFF voltages, 0.5 V, 0.4 V, 0.3 V, and 0.1 V.

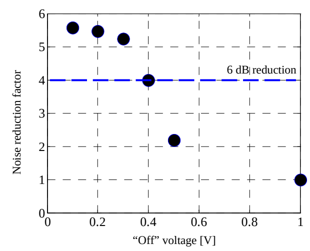

Fig. 10: Noise reduction factor for different OFF voltages. The oxide-trapping model is used.

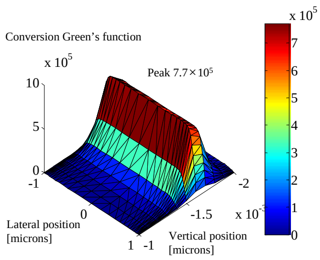

Fig. 11: Real part of the drain current conversion Green’s function (from baseband to baseband) for the oxide trap continuity equation in the oxide trap region.

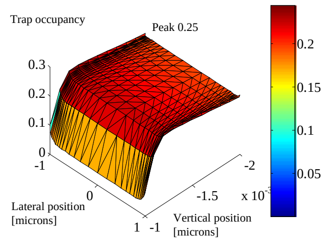

Fig. 12: Trap occupancy at 0.05 msec, when the OFF voltage is 0.5 V. The peak value is about 0.25.

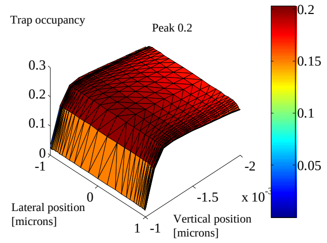

Fig. 13: Trap occupancy at 0.05 msec, when the OFF voltage is 0.1 V. The peak value is about 0.2.

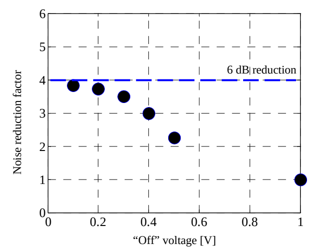

Fig. 14: Noise reduction factor for different OFF voltages. Hooge’s model is used.

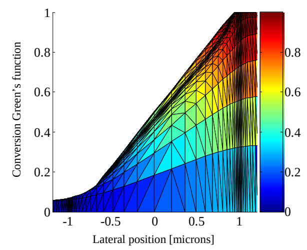

Fig. 15: Real part of the drain current conversion Green’s function (from baseband to baseband) for the electron continuity equation. The OFF voltage is 0.1 V.